THE JOURNAL OF CHEMICAL PHYSICS **138**, 134701 (2013)

Extension of the Test-Area methodology for calculating solid-fluid interfacial tensions in cylindrical geometry

Felipe J. Blas[1,2,a)] and Bruno Mendiboure[3,b)]
[1]*Departamento de Física Aplicada, Universidad de Huelva, 21071 Huelva, Spain*
[2]*Centro de Investigación de Física Teórica y Matemática FIMAT, Universidad de Huelva, 21071 Huelva, Spain*
[3]*Laboratoire des Fluides Complexes et leurs Réservoirs, UMR5150, Université de Pau et des Pays de l'Adour, B. P. 1155, Pau Cedex 64014, France*

(Received 21 December 2012; accepted 7 March 2013; published online 1 April 2013)

We extend the well-known Test-Area methodology of Gloor *et al.* [J. Chem. Phys. **123**, 134703 (2005)], originally proposed to evaluate the surface tension of planar fluid-fluid interfaces along a computer simulation in the canonical ensemble, to deal with the solid-fluid interfacial tension of systems adsorbed on cylindrical pores. The common method used to evaluate the solid-fluid interfacial tension invokes the mechanical relation in terms of the tangential and normal components of the pressure tensor relative to the interface. Unfortunately, this procedure is difficult to implement in the case of cylindrical geometry, and particularly complex in case of nonspherical molecules. Following the original work of Gloor *et al.*, we perform free-energy perturbations due to virtual changes in the solid-fluid surface. In this particular case, the radius and length of the cylindrical pore are varied to ensure constant-volume virtual changes of the solid-fluid surface area along the simulation. We apply the modified methodology for determining the interfacial tension of a system of spherical Lennard-Jones molecules adsorbed inside cylindrical pores that interact with fluid molecules through the generalized 10-4-3 Steele potential recently proposed by Siderius and Gelb [J. Chem. Phys. **135**, 084703 (2011)]. We analyze the effect of pore diameter, density of adsorbed molecules, and fluid-fluid cutoff distance of the Lennard-Jones intermolecular potential on the solid-fluid interfacial tension. This extension, as the original Test-Area formulation, offers clear advantages over the classical mechanical route of computational efficiency, easy of implementation, and generality.
 [http://dx.doi.org/10.1063/1.4795836]

I. INTRODUCTION

During the last years there has been a great advance in the understanding of the interfacial properties of inhomogeneous systems from a molecular perspective. This knowledge is not ascribed only to the cases of vapour-liquid and liquid-liquid (free) interfaces, but also to other inhomogeneous situations, including systems formed by molecules near planar walls, inside slit-like pores, as well as cylindrical pores and spherical cavities, and in general, to all situations concerning fluids adsorbed on structured materials as zeolites, nanotubes, and amorphous adsorbents. These are only a few examples of systems for which new methods of Statistical Mechanics and computer simulation techniques are now available to describe their thermodynamic and structural behaviour.

This advance is due to the continuous development of Statistical Mechanics molecular-based theories. The rapid development of Density Gradient Theory (DGT)[1–7] and Density Functional Theory (DFT)[8,9] allows us to determine thermodynamic and structural properties of spherical and molecular inhomogeneous systems. Particularly relevant to this discussion are the works published for predicting and understanding the behaviour of fluids at free interfaces and adsorbed on different materials. The new generation of functional theories, such as those based on Fundamental Measure Theory (FMT)[10–12] and their different versions, have provided an important insight in the field. We recommend the works of Llovell *et al.*[13] for a recent review of the literature, as well as the recent work of Malijevský and Jackson[14] on the determination of the interfacial properties of nanoscopic liquid drops.

Computer simulation methods have also experienced a great development in the field of interfacial properties, particularly due to the appearance of new techniques for calculating fluid-fluid interfacial tension. The traditional method used for determining this key property has been (and still is) the mechanical route, through the evaluation of the microscopic components of the pressure tensor from the virial. The first explicit expression of the local pressure tensor for a planar vapour-liquid interface was proposed by Irving and Kirkwood in 1950.[15] This method is based on the well-known mechanical or virial route for the determination of the pressure. Alternatively, Harasima proposed a different but also valid expression for the local tangential pressure several years later.[16] However, although the calculation of the interfacial tension, as well as the pressure tensor components, is always possible via the mechanical or virial route, care has to be taken in the case of systems interacting through discontinuous potentials due to the impulsive forces and the corresponding delta functions associated to the virial. These contributions must be

a)Electronic mail: felipe@uhu.es
b)This work was developed during a visit in Departamento de Física Aplicada and Centro de Investigación de Física Teórica y Matemática FIMAT of Universidad de Huelva.

calculated accurately, as shown by Allen[17] and more recently by de Miguel and Jackson[18] and Brumby *et al.*[19]

As mentioned previously, during the last decade there has been an intense and fruitful development of new methodologies based on the thermodynamic definition of surface tension. The use of new theoretical approaches, such as the Expanded Ensemble,[20,21] Wandering Interface Method,[22] or perturbative methods as the Test-Area (TA)[23] technique, or the determination of the macroscopic components of the pressure tensor (using for instance virtual volume changes, as proposed by de Miguel and Jackson[18,24] or Brumby *et al.*[19]), are only a few examples of the new methods available in the literature from a computer simulation perspective. These methods are becoming very popular, and as an example the TA method has been so far used by several authors to determine vapour-liquid interfacial properties of fully-flexible Lennard-Jones (LJ) chains,[25] linear-tangent LJ chains,[26,27] several models of water,[28–30] the Mie potential,[5,31] or binary fluid mixtures.[7,32,33]

The mechanical and thermodynamic methods have been applied for determining the fluid-fluid (mainly vapour-liquid) surface tension of simple and complex systems using Monte Carlo and Molecular Dynamics computer simulations. However, this is not the case when dealing with confined inhomogenous systems. There are only a few studies in which the solid-fluid (SF) interfacial tension of molecules confined in planar geometries, such as slit-like pores, is calculated from computer simulation (see, for instance, the works of Henderson and van Swol,[34] Heni and Löwen,[35] Varnik *et al.*,[36] Fortini *et al.*,[37] Hamada *et al.*,[38] Singh and Kwak,[39] and Das and Binder[40]), while most authors concentrate on phase behaviour,[41] adsorption,[42] or fluid structure.[43] This is because the SF interfacial tension of confined substances is not experimentally accessible. However, its determination is important from a formal point of view because this quantity is easily calculated theoretically from DFT. A comparison between theoretical and computer simulation predictions constitutes a strong test to check the ability of a theory in predicting the behaviour of adsorbed molecules in a pore.[44]

From a technical point of view, the calculation of the SF interfacial tension, as well as the normal and tangential components of the pressure tensor of fluids confined in slit-like pores, is not a difficult task. In fact, this can be done easily evaluating the local pressure tensor components through the mechanical (virial) route of Irving and Kirkwood[15] or Harasima.[16] For a system confined inside a slit-like pore, the molecules are located between two parallel walls that interact with the fluid via a known SF intermolecular potential. The z-axis is chosen perpendicular to the walls of the pore and the x-axis and y-axis are parallel to the walls. It is important to recall here that in a inhomogeneous system the pressure is not a scalar but a tensorial quantity. In the particular case of pores with planar geometry in which the inhomogeneity of the system is along the direction perpendicular to the walls, i.e., the z-axis, the microscopic perpendicular or normal (along the z-axis direction) component of the pressure tensor, $P_{zz} \equiv P_{\mathrm{N}}$, is constant and equal to the "true" thermodynamic pressure inside the pore. The microscopic tangential components of the pressure tensor, parallel to the walls, $P_{xx}(z) = P_{yy}(z) \equiv P_{\mathrm{T}}(z)$, are functions of the z coordinate or distance to the walls, and it is different to P_{N}, i.e., $P_{\mathrm{T}}(z) \neq P_{\mathrm{N}}$. Obviously, this is exactly the same scenario as in vapour-liquid and liquid-liquid (free) interfaces. Care must be taken however in this particular case since an extra contribution to the normal component of the pressure tensor must be considered. Note that the tangential component is also calculated as in the case of planar free interfaces since the wall potential acts only in the z-direction along which the system exhibits the inhomogeneity. For further details see the work of Varnik *et al.*[36] and references therein.

The number of papers devoted to study the interfacial tension and the determination of the components of the pressure tensor of a fluid confined in a cylindrical pore are even more scarce, probably due to the mathematical difficulties in solving the corresponding equations. It is important to recall here that, contrary to what happens in problems involving planar geometries, the normal component of the pressure tensor in cylindrical geometry is no longer constant along the radial direction (perpendicular to the SF interface). There exist studies on vapour-liquid (free) cylindrical interfaces using both theory and computer simulation, such as the works of Lovett and co-workers[45–47] and Thompson *et al.*[48] As previously mentioned, the rapid development of the DFT formalisms, with particular emphasis on the FMT approaches, has allowed us to study the adsorption and structural behaviour of fluids adsorbed in cylindrical pores.[49,50] However, to our knowledge, there are no studies in which the SF interfacial tension of fluids adsorbed in cylindrical pores is evaluated from computer simulation.

The goal of this work is to generalize the TA technique to deal with SF interfacial tensions of molecules confined in cylindrical pores. The method is extended using the appropriate virtual or perturbative changes in the SF interfacial area keeping the volume of the system constant, as in the original approach.[23] The new technique is validated considering different relative SF surface area changes in a range of small values and then extrapolating the interfacial tension values to zero. We have also applied the methodology proposed to investigate the effect of pore diameter, fluid-fluid cutoff distance associated to the corresponding intermolecular potential, and system size on the SF interfacial tension. To our knowledge, this is the first time this interfacial property is determined using a perturbative method from computer simulation.

The rest of the paper is structured as follows. In Sec. II we derive the extension of the formalism for determining the SF interfacial tension of molecules inside cylindrical pores. Section III presents the models and simulation details and in Sec. IV we discuss the results obtained. Finally, we present the main conclusions of this work.

II. TEST-AREA METHODOLOGY FOR CYLINDRICAL GEOMETRY

Consider a system of N particles at a given temperature T and occupying a cylinder of volume V. In the canonical or NVT ensemble, the key free energy is the Helmholtz energy $F = F(N, V, T) \equiv F_{NVT}$. The variation in Helmholtz free energy when the temperature, volume, and number of

particles are changed with their corresponding infinitesimal amounts is given by the well-known change of free energy in the canonical ensemble. However, density variations produce an extra contribution to the thermodynamic state functions in general, and to the Helmholtz free energy in particular. In the presence of an interface the free energies and particularly F need to be modified to include the work that has to be imposed by external forces in order to change the interfacial area $\mathcal{A}$ by $d\mathcal{A}$,

$$dF(\mathcal{A}) = -SdT - PdV + \mu dN + \gamma d\mathcal{A}. \tag{1}$$

The contribution $\gamma d\mathcal{A}$ is the work needed to change the interfacial area a differential amount $d\mathcal{A}$, at constant temperature, volume, and number of particles, and the coefficient γ is the interfacial tension of the system. Note that now $F = F(N, V, T, \mathcal{A}) \equiv F_{NVT}(\mathcal{A})$ is also a function of the interfacial area $\mathcal{A}$. Its thermodynamic definition follows from the expression,

$$\gamma = \left(\frac{\partial F}{\partial \mathcal{A}}\right)_{NVT}, \tag{2}$$

where the partial derivative must be evaluated at constant number of particles N, volume V, and temperature T.

Similarly to the case of the planar geometry, the interfacial tension can be computed efficiently from the previous expression by using fictitious increasing and decreasing surface area. The Helmholtz free energy is related with the canonical partition function Q_{NVT} through the well-known Statistical Mechanics relationship,

$$F \equiv F_{NVT}(\mathcal{A}) = -k_B T \ln Q_{NVT}, \tag{3}$$

where k_B is Boltzmann's constant. The canonical partition function of a system of N spherical molecules without internal degrees of freedom, at temperature T and volume V, can be written as

$$Q_{NVT} = \frac{1}{\Lambda^{3N} N!} \int d\mathbf{r}^N \exp[-\beta U_N(\mathbf{r}^N)] = \frac{1}{\Lambda^{3N} N!} Z_{NVT}, \tag{4}$$

where Λ is the de Broglie wavelength associated to the translational degrees of freedom of the system, $U_N \equiv U_N(\mathbf{r}^N)$, the intermolecular potential energy of a system formed by N particles that depends on all the positions $\mathbf{r}^N \equiv \{\mathbf{r}_1, \ldots, \mathbf{r}_N\}$, $\beta = (k_B T)^{-1}$, and Z_{NVT} is the configurational partition function of the system

$$Z_{NVT} = \int d\mathbf{r}^N \exp[-\beta U_N(\mathbf{r}^N)]. \tag{5}$$

Although we have explicitly used the relationship given by Eq. (4) valid for systems that interact through spherical intermolecular potentials, with no internal degrees of freedom, the methodology is equally applicable to molecular systems.

Perturbative methods in computer simulation allow to calculate a number of thermodynamic properties from estimation of the change in the appropriate free energy under fictitious perturbation. The works of Eppenga and Frenkel,[51] Harismiadis *et al.*,[52] and de Miguel and Jackson,[18,24] in the case of pressure or components of the pressure tensor, and that of Gloor *et al.*[23] in the case of surface tension, are clear examples of this methodology. Following the work of Gloor *et al.*,[23] the interfacial tension can be easily evaluated in the canonical ensemble using the appropriate thermodynamics definition. Using Eq. (2), the interfacial tension, in the reference state, can be expressed as the difference in Helmholtz free energy between two states with different surface areas,

$$\gamma = \left(\frac{\partial F}{\partial \mathcal{A}}\right)_{NVT} = \lim_{\Delta\mathcal{A}\to 0} \frac{F_{NVT}(\mathcal{A}_0 + \Delta\mathcal{A}) - F_{NVT}(\mathcal{A}_0)}{\Delta\mathcal{A}} \approx \frac{\Delta F_{NVT}}{\Delta\mathcal{A}}, \tag{6}$$

where $\mathcal{A}_0$ is the interfacial area of the reference state and $\mathcal{A}_1 \equiv \mathcal{A}_0 + \Delta\mathcal{A}$ the interfacial area of the perturbed state. Since the TA methodology has been presented and applied elsewhere, here we only give the key final expressions of this technique. For further details we recommend the original works.

The difference in Helmholtz free energy is proportional to the logarithm of the average of the Boltzmann factor associated to the surface area perturbation over the unperturbed system of surface area $\mathcal{A}_0$. This configurational average can be written as

$$\Delta F_{NVT} = -k_B T \ln \langle \exp[-\beta \Delta U^+] \rangle_{NVT}, \tag{7}$$

where $\Delta U^+ = U(\mathcal{A}_1) - U(\mathcal{A}_0) \equiv U(\mathcal{A}_0 + \Delta\mathcal{A}) - U(\mathcal{A}_0)$ is the change in potential energy when the interfacial area changes from $\mathcal{A}_0$ to $\mathcal{A}_1 \equiv \mathcal{A}_0 + \Delta\mathcal{A}$. The final expression of the interfacial tension is then

$$\gamma^+ = -\frac{k_B T}{\Delta\mathcal{A}} \ln \langle \exp[-\beta \Delta U^+] \rangle_{NVT}. \tag{8}$$

In principle, one could also have selected a backward, finite difference scheme to approximate the first derivative of the free energy. In this case one can write

$$\gamma = \left(\frac{\partial F}{\partial \mathcal{A}}\right)_{NVT} = \lim_{\Delta\mathcal{A}\to 0} \frac{F_{NVT}(\mathcal{A}_0 - |\Delta\mathcal{A}|) - F_{NVT}(\mathcal{A}_0)}{|\Delta\mathcal{A}|} \tag{9}$$

which results in an expression for the interfacial tension of the form

$$\gamma^- = -\frac{k_B T}{|\Delta\mathcal{A}|} \ln \langle \exp[-\beta \Delta U^-] \rangle_{NVT}, \tag{10}$$

where $\Delta U^- = U(\mathcal{A}_1) - U(\mathcal{A}_0) \equiv U(\mathcal{A}_0 - |\Delta\mathcal{A}|) - U(\mathcal{A}_0)$ is the change in potential energy when the interfacial area changes from $\mathcal{A}_0$ to $\mathcal{A}_1 \equiv \mathcal{A}_0 - |\Delta\mathcal{A}|$.

For systems of particles interacting through continuous potentials, γ^+ and γ^- are expected to be equal to the value of the interfacial tension as long as $\Delta\mathcal{A} \to 0$. In practical implementations, small but finite values of $\Delta\mathcal{A}$ must be used, and the forward and backward approaches will not yield exactly the same value. Once independent values of surface tension for the positive and negative change in SF interfacial area are obtained from Eqs. (8) and (10) for several values of the perturbation parameter, the final estimate of the SF interfacial tension is determined from an extrapolation to $\Delta\mathcal{A} \to 0$ with linear fit of the averages obtained for the different values of $\Delta\mathcal{A}$.

As in previous works,[18,21,23–25,28,29,33,53] the central finite-difference approximation should provide a more reliable estimate of the derivative given by Eqs. (6) and (9). In this case, the interfacial tension can be expressed as

$$\gamma = \frac{\gamma^+ + \gamma^-}{2}, \tag{11}$$

where γ^+ and γ^- are given by Eqs. (8) and (10), respectively. Special care must be taken when using Eq. (11) for determining the interfacial tension of systems that interact through non-continuous intermolecular interactions. The use of Eq. (11) assumes implicitly that both increasing and decreasing surface area perturbations are appropriate to gauge the value of interfacial tension. This is not expected for systems with discontinuous intermolecular potentials, as was first noted by Eppenga and Frenkel[51] some years ago, and more recently by de Miguel and co-workers.[18,19,24] However, as we deal with continuous intermolecular potentials, the use of Eqs. (8), (10) and (11) is fully justified from a theoretical point of view.

In this work we extend the TA methodology for dealing with SF interfaces. Here we briefly give the most important technical details of this extension. Our inhomogeneous system consists of a fluid (gas or liquid) in direct contact with the solid phase of a substrate that acts as adsorbent. In other words, in the reference state the fluid phase is contained within a cylindrical simulation box of volume

$$V_0 = \pi R_0^2 H_0, \tag{12}$$

where R_0 is the pore radius in the reference state. If the z-axis is chosen along the symmetry axis of the cylinder, H_0 is the dimension of the simulation box along the z-axis in the reference state.

Following the original work of Gloor *et al.*,[23] we assume that $\mathcal{A}_0$, the SF interfacial area of the reference state, may be written as

$$\mathcal{A}_0 = 2\pi R_0 H_0, \tag{13}$$

where R_0 and H_0 are the radius and length along the z-axis of the simulation box in the reference state. The appropriate dimensionless perturbation parameter ξ, set at the start of the simulation, is defined as usually, i.e., $\xi = \Delta\mathcal{A}/\mathcal{A}_0$, where $\mathcal{A}_0$ is given by Eq. (13) and $\Delta\mathcal{A}$ is a (small) change in the SF interfacial area, which in this particular case corresponds to the lateral area of the cylindrical simulation box, $\Delta\mathcal{A} = \mathcal{A}_1 - \mathcal{A}_0$. The interfacial area after a virtual change of the lateral area may be written as $\mathcal{A}_1 = \mathcal{A}_0(1+\xi)$. The volume of the system in the perturbed state, V_1, may be written in terms of the interfacial area $\mathcal{A}_1 = 2\pi R_1 H_1$ as

$$V_1 = \pi R_1^2 H_1 = \pi R_1^2 \left(\frac{\mathcal{A}_1}{2\pi R_1}\right) = \frac{1}{2} R_1 \mathcal{A}_1. \tag{14}$$

Since we are using the original TA methodology developed for simulations carried out in the canonical or NVT ensemble, one possibility is to perform perturbations in such a way that the scaled dimension along the radial dimension axis is decreased. This corresponds to positive values of ξ and $\Delta\mathcal{A}$, meaning that the SF interfacial area is increased. Under this hypothesis, the radial dimension in the perturbed state is given by

$$R_1 = R_0(1+\xi)^{-1}. \tag{15}$$

To keep the overall volume constant, for the case $\xi = \Delta\mathcal{A}/\mathcal{A}_0 > 0$, the dimension in the axial or z direction is increased according to

$$H_1 = H_0(1+\xi)^2. \tag{16}$$

It is easy to demonstrate that the choice of Eqs. (15) and (16) corresponds to a new SF surface area given by $\mathcal{A}_1 = \mathcal{A}_0(1+\xi)$. Other choices for R_1 and H_1 are however possible although in this work we only used the recipes given by the last two equations.

The procedure described above corresponds to positive TA perturbations, in such a way that the SF interfacial area is increased, $\Delta\mathcal{A} \equiv \mathcal{A}_1 - \mathcal{A}_0 > 0$. Note that the positive TA perturbation implies that the radius of the cylindrical box is decreased and the dimension along the z-axis of the cylinder is increased. In the same way as in the original TA methodology,[23] negative perturbations are also possible here. In this case, the dimensionless parameter ξ is negative, $\xi = -|\Delta\mathcal{A}|/\mathcal{A}_0$. According to that, the radius and the dimension along the z-axis are increased and decreased, respectively, using the following expressions

$$R_1 = R_0(1-|\xi|)^{-1} \tag{17}$$

and

$$H_1 = H_0(1-|\xi|)^2. \tag{18}$$

As in previous works, positive and negative perturbations are undertaken simultaneously once every Monte Carlo cycle to evaluate the Boltzmann factors associated to the difference in configurational energy which are required to determine the change in free energy and the SF interfacial tension.

III. MODELS AND SIMULATION DETAILS

We have applied the methodology proposed in Sec. II to study the SF interfacial tension of a simple fluid confined inside cylindrical pores. In particular, the pores considered in this work are cylinders that mimic the SF Steele 10-4-3 potential. The molecules confined inside these pores are spherical molecules whose intermolecular interaction energy is described through the classical Lennard-Jones (LJ) potential:

$$u_{ff}(r_{ij}) = 4\epsilon_{ff}\left[\left(\frac{\sigma_{ff}}{r_{ij}}\right)^{12} - \left(\frac{\sigma_{ff}}{r_{ij}}\right)^{6}\right], \tag{19}$$

where $u_{ff}(r_{ij})$ is the intermolecular potential energy between particles i and j that depends only on the distance between the centers of molecules $r_{ij} \equiv |\mathbf{r}_i - \mathbf{r}_j|$. The interactions are spherically truncated but not shifted at a given distance r_c. No long-range corrections are applied and all the calculations are carried out considering two different cutoff distances, $r_c = 2.5$ and $4.5\sigma_{ff}$. As it is well known, σ_{ff} stands for the diameter of the molecular spherical core, and ϵ_{ff} is the depth of the pairwise interaction potential. The subscript ff stands for fluid-fluid molecular interactions. The confinement

of LJ spheres inside cylindrical pores of the characteristics explained in this work has been recently studied using DFT by Siderius and Gelb.[54]

The LJ molecules interact with the cylindrical wall. Among the extensive collection of models proposed in literature to account for SF molecular interactions, the so-called Steele[55] 10-4-3 potential is very popular as it has been used to reproduce the interaction with realistic planar solid substrates. This model considers that the atoms constituting the solid substrate are placed in layers equispaced by a distance Δ, and placed in parallel to the SF dividing surface. Each of the solid substrate atoms is supposed to interact with every individual fluid molecule through a LJ potential. According to Siderius and Gelb,[54] a cylindrical analog of the 10-4-3 Steele potential models a material composed of a continuous cylindrical surface of radius R formed by atoms that interact with the fluid molecules through the classical LJ intermolecular potential. In addition to that, the pores have a continuum cylindrical surface of radius R with a real density ρ_A, composed of atoms that interact with the fluid through the LJ potential, and a continuum slab of material that begins at position $r = R + \alpha\Delta$ and extends to $R \to \infty$, of volume density ρ_S, composed of atoms that interact with the molecules via the attractive portion of the LJ potential. It is important to recall here that α is an empirical, positive-value parameter, as in the case of the original planar 10-4-3 Steele potential. Following Siderius and Gelb, $\rho_A = \rho_S\Delta$ and the total interaction between a fluid molecule and the cylindrical wall is written as[54]

$$u_{sf}(r, R) = 2\pi\rho_S\Delta\sigma_{sf}^2\epsilon_{sf}\left[\psi_6(r, R, \sigma_{sf}) - \psi_3(r, R, \sigma_{sf}) - \frac{\sigma_{sf}}{\Delta}\phi_3(r, R + \alpha\Delta, \sigma_{sf})\right], \tag{20}$$

where r is the distance from the center of the cylindrical pore to the position of the molecule inside it, R is the pore radius, and $\psi_n(r, R, \sigma_{sf})$ and $\phi_n(r, R, \sigma_{sf})$ are given by

$$\psi_n(r, R, \sigma_{sf}) = 4\sqrt{\pi}\frac{\Gamma(n - \frac{1}{2})}{\Gamma(n)}\left(\frac{\sigma_{sf}}{R}\right)^{2n-2}\left[1 - \left(\frac{r}{R}\right)^2\right]^{2-2n} \times F\left[\frac{3-2n}{2}, \frac{3-2n}{2}; 1; \left(\frac{r}{R}\right)^2\right] \tag{21}$$

and

$$\phi_n(r, R, \sigma_{sf}) = \frac{4\sqrt{\pi}}{2n-3}\frac{\Gamma(n-\frac{1}{2})}{\Gamma(n)}\left(\frac{\sigma_{sf}}{R}\right)^{2n-3}\left[1-\left(\frac{r}{R}\right)^2\right]^{3-2n} \times F\left[\frac{3-2n}{2}, \frac{5-2n}{2}; 1; \left(\frac{r}{R}\right)^2\right]. \tag{22}$$

Γ is the Gamma function and F is the hypergeometric function. Note that n must be either an integer or half-integer greater that 1/2. Following the works of Siderius and Gelb[54] and Steele,[55] the typical graphite values of ρ_S and Δ are used here, i.e., $\rho_S = 114.0\,\text{nm}^{-3}$ and $\Delta = 0.335\,\text{nm}$. The α parameter may be tuned to match some particular material, but according to Siderius and Gelb,[54] we use $\alpha = 0.61$ to be consistent with the planar Steele 10-4-3 potential. σ_{sf} and ϵ_{sf} are the molecular size and dispersive energy associated to the LJ intermolecular interaction between a fluid molecule and a single constituent particle of the solid. These parameters are calculated using the usual Lorentz-Berthelot combining rules, i.e., $\sigma_{sf} = \frac{1}{2}(\sigma_{ss} + \sigma_{ff})$ and $\epsilon_{sf} = (\epsilon_{ss}\epsilon_{ff})^{1/2}$. For calculating σ_{sf} and ϵ_{sf} is necessary to find the molecular parameters of the LJ units of the solid and the absorbed fluid. In our work, the spherical molecules forming the cylindrical wall are carbon units that model graphite, for which we use the original values of Steele $\sigma_{ss} = 0.340\,\text{nm}$ and $\epsilon_{ss}/k_B = 28.0\,\text{K}$, and the spherical LJ molecules of the fluid are modelled as methane, i.e., $\sigma_{ff} = 0.37327\,\text{nm}$ and $\epsilon_{ff}/k_B = 149.92\,\text{K}$.[56]

We apply the methodology presented in Sec. II to determine the SF interfacial tension of a system of spherical molecules contained in cylindrical pores with different pore radius, number of adsorbed molecules, and densities inside the pore. In particular, we consider systems containing $N = 500$ and 1000 spherical molecules interacting with other molecules through the Lennard-Jones intermolecular potential and with the walls of the pore according to the generalization of the 10-4-3 Steele potential, as discussed previously.

Simulations are performed in the canonical or NVT ensemble. We consider a system of N molecules at a temperature T in a volume $V = \pi R^2 H$, where R and H are the pore radius and the dimension of the cylindrical box along the z-axis, respectively. Initially, N Lennard-Jones molecules are placed inside the cylindrical simulation box at positions randomly selected. This procedure ensures that simulations are run at the desired (and fixed) density.

The simulations are organized in cycles. A cycle is defined as N trial moves (displacement of the center of the molecule). The magnitude of the appropriate displacement is adjusted so as to get an acceptance rate of 30% approximately. We use periodic boundary conditions and minimum image convention along the z-axis of the simulation box (direction of the axis of the cylinder). A typical run consisted of 2×10^6 equilibration cycles followed by a production stage of at least 2×10^6 cycles. During this last stage averages of the desired interfacial properties were computed, including density profiles and SF interfacial tension. Simulation box profiles along the r-axis direction were determined by dividing the cylindrical box in 100 concentric cylindrical shells with equal width along the radial direction. The production stage is divided into blocks. The ensemble averages of the SF interfacial tension, for several relative surface area changes $\xi = \Delta\mathcal{A}/\mathcal{A}_0$ in the range $10^{-4} \leq |\xi| \leq 10 \times 10^4$ (see Sec. IV and Figs. 2–4 for further details), are obtained from the arithmetic mean of the block averages, and the statistical precision of the sample averages are estimated from the standard deviation of the mean.[57] From this information, the final SF interfacial tension values are obtained by linear regression to $|\xi| \to 0$ of the values obtained from increasing-area (γ^{+}*) and decreasing-area (γ^{-}*) perturbations, and a combined increasing-decreasing (γ*) perturbation given by Eq. (11). Results presented for the final SF interfacial tension values and their corresponding estimates of the statistical precision correspond to the errors associated to the linear extrapolations. We have compared the uncertainties obtained from block averaging and linear extrapolation and checked carefully that the relative sizes of both of them are equivalent and of the same order of magnitude.

IV. RESULTS

We now turn to analyze the adequacy of the extension of the TA methodology presented in Sec. II for the determination of the SF interfacial tension of fluids confined in cylindrical geometry. In the following discussion, the fluid-fluid dispersive energy parameter ε_{ff} and the diameter σ_{ff} are chosen as the units of energy and length, respectively. According to this, we define the following reduced quantities: temperature, $T^* = k_B T/\varepsilon_{ff}$; bulk number density and density profile, $\rho^* = \rho\sigma_{ff}^3$ and $\rho^*(r^*) = \rho(r^*)\sigma_{ff}^3$; surface tension, $\gamma^* = \gamma\sigma_{ff}^2/\varepsilon_{ff}$; pore diameter, $R^* = R/\sigma_{ff}$; length of the simulation box along the z-axis (direction of the symmetry axis of the cylinder), $L_z^* = L_z/\sigma_{ff}$; distance from the center of the cylinder, $r^* = r/\sigma_{ff}$; and fluid-fluid cutoff distance, $r_c^* = r_c/\sigma_{ff}$.

We first consider systems of $N = 500$ LJ molecules in cylindrical pores of fixed radius $R^* = 7.5$ and length along the symmetry axis $L_z^* = 15$ ($\rho^* = 0.1886$), $L_z^* = 10$ ($\rho^* = 0.2829$), $L_z^* = 8.8$ ($\rho^* = 0.3215$), and $L_z^* = 7.5$ ($\rho^* = 0.3773$). We also consider systems of $N = 1000$, $R^* = 7.5$, and $L_z^* = 8.8$ ($\rho^* = 0.6431$). All the systems considered are studied at a fixed temperature of $T^* = 2.0$, which corresponds to supercritical fluid states in the bulk. Two cases are analyzed: we first consider fluid-fluid interactions spherically truncated (but non-shifted) at a cutoff distance $r_c^* = 4.5$; after, we consider interactions spherically truncated and non-shifted, but the fluid-fluid cutoff distance is now $r_c^* = 2.5$. This allows us to check the effect of the long-range corrections of the fluid-fluid intermolecular LJ potential on the determination of the SF interfacial properties.

We have used the methodology explained in Sec. II to obtain the SF interfacial tension of the system using the two cutoff distances mentioned previously. In addition to that, we have also obtained the density profiles of the molecules adsorbed inside the pore. In Fig. 1 we present the density profiles of LJ molecules adsorbed inside two different cylindrical pores that interact with the wall through the 10-4-3 Steele interaction potential described in Sec. III. Results presented here correspond to simulations performed with $N = 500$ molecules. We have also simulated larger systems formed by $N = 1000$ LJ spheres, but since the results corresponding to density profiles are nearly identical, we have not represented them. We have also compared the density profiles for molecules with different cutoff distances, $r_c^* = 4.5$ and 2.5. Comparison between both density profiles indicate that differences are fully negligible. We have considered, as previously mentioned, systems of LJ molecules with different number densities inside the cylindrical pore of radius $R^* = 7.5$. As can be seen in part (a) of the figure, the system develops different adsorbed layers inside the pore depending on the number density of the system. In particular, molecules tend to be preferentially adsorbed close to the cylindrical wall, forming a ring of molecules adsorbed. As the distance from the center of the pore decreases the height of the peaks associated to the corresponding density profile also decreases, observing a nearly flat density profile around the center of the cylinder, as expected. This indicates that SF interactions are negligible for molecules located in this region and hence, a bulk-like behaviour of the system is exhibited there. At $\rho^* = 0.1886$, the system develops only a dense ring layer at $r^* \approx 6.5$, and a second but much smaller adsorption peak at $r^* \approx 5.5$, approximately. As the number density inside the pore increases, from $\rho^* = 0.2829$ up to 0.3773, the two adsorption peaks become higher, and eventually, a third adsorption ring layer appear at $r^* \approx 4.5$, as expected. For even denser systems, i.e., $\rho^* = 0.6431$, the molecules distribute inside the pore in 6–7 ring layers. Note that oscillations of the density profile due to correlations provoked by the confinement of molecules inside the pore are present along the whole cylinder, including its central region.

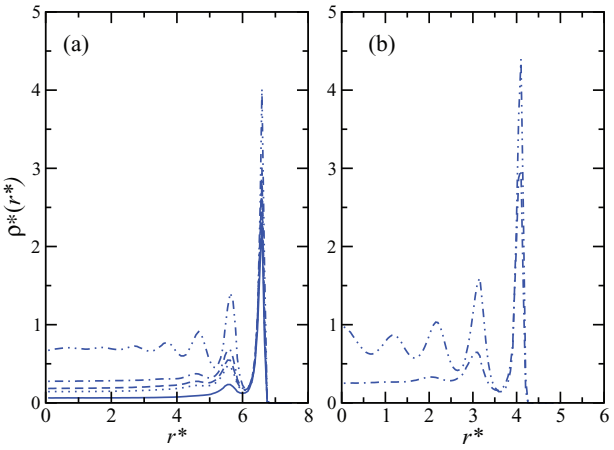

FIG. 1. Density profiles of LJ molecules adsorbed on cylindrical pores with pore radius (a) $R^* = 7.5$ and (b) $R^* = 5.0$ at $T^* = 2.0$ obtained from MC NVT simulations. The curves correspond to total densities inside the cylindrical pore of $\rho^* = 0.1886$ (continuous line), 0.2829 (dotted line), 0.3215 (dashed line), 0.3773 (dotted-dashed line), and 0.6431 (dotted-dotted-dashed line).

We have also considered the adsorption behaviour of LJ molecules inside a thinner cylindrical pore of radius $R^* = 5.0$, considering the cutoff distances previously used, namely, $r_c^* = 4.5$ and 2.5. Since the main goal of this work is to check the ability of the generalization of the TA methodology in predicting the SF interfacial tension in cylindrical geometry, we only concentrate only in systems of $N = 500$ molecules in a cylindrical pore of length along the symmetry axis $L_z^* = 16.85$ and number density $\rho^* = 0.3778$, $L_z^* = 10$ and number density $\rho^* = 0.6366$, and reduced temperature of $T^* = 2.0$. As in the case of the adsorption in wider pores, the density profiles of LJ molecules with different cutoff distances are indistinguishable, an expected result for systems in which the SF interactions dominate its behaviour. At the lowest density ($\rho^* = 0.3778$), the density profile exhibits three peaks at $r^* \approx 4$, 3, and 2, and bulk-like behaviour in the central part of the cylinder. At the highest density, $\rho^* = 0.6366$, the density profile shows five different adsorbed (ring-like) layers. In particular, the density profile shows the expected oscillatory behaviour as the distance from the center of the cylinder is varied, similar to that found at approximately the same density in the cylinder of pore $R^* = 7.5$. An interesting behaviour exhibited by the system in narrower pores is the existence of an adsorbed layer of molecules located exactly at the center of the cylinder. This expected behaviour is a

consequence of the cylindrical geometry, as observed previously by several authors.[49]

Once the structural behaviour of the LJ fluid inside the pore is well characterized in terms of the density profiles, we present the simulation data for the SF interfacial tension of the system of $N = 500$ LJ molecules, with $r_c^* = 4.5$, at $T^* = 2.0$, adsorbed inside a cylindrical pore of radius $R^* = 7.5$. Interfacial tension is obtained from Eqs. (8), (10), and (11) for relative SF surface changes $|\xi| = \Delta\mathcal{A}/\mathcal{A}$ in the range $10^{-4} \leq |\xi| \leq 10 \times 10^{-4}$. We use the methodology previously described in Sec. II. In particular, the virtual surface area perturbations of magnitude ξ are performed every cycle by rescaling the radius and box length along the z-axis according to Eqs. (15)–(18). Following the original methodology, the positions of the molecular centers of mass are also calculated according to the transformations $r' = (1 \pm |\xi|)^{-1} r$ and $z' = (1 \pm |\xi|)^2 z$. Here r and z (and r' and z') are the radial and z-axis cylindrical coordinates of the molecules, respectively. Note that, as is the original TA[23] and their different extensions,[5,7,24–29,31–33,44] r_c remains unchanged under this transformation.

It is clear from Fig. 2 that surface tension exhibits a definite linear behaviour over the range of values of ξ considered here for all the densities studied. The set of data obtained from both increasing and decreasing perturbations of the SF surface are extrapolated cleanly to the same value γ^*, for each of the densities considered, when $|\xi| \to 0$. Results corresponding to the five densities are also presented in Table I. Note that for $\rho^* = 0.6431$ we have performed simulations only for $N = 1000$ LJ molecules, but not for $N = 500$ particles. As can be seen, the SF interfacial tension becomes more negative as the density inside the cylindrical pore is larger. This is the expected behaviour since the SF cohesion energy increases as the density of the adsorbed phase is increased. However, this trend is not followed when increasing the density from

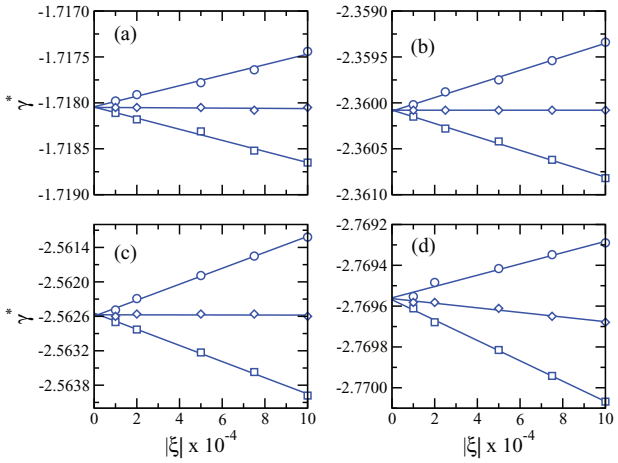

FIG. 2. Interfacial tension for the SF interface in a system of $N = 500$ LJ molecules adsorbed on a cylindrical pore of radius $R^* = 7.5$ as obtained from surface area perturbations in MC *NVT* simulations with fluid-fluid interaction cutoff distance at $r_c^* = 4.5$. The reduced temperature is $T^* = 2.0$ and density inside the cylindrical pore is (a) $\rho^* = 0.1886$, (b) $\rho^* = 0.2829$, (c) $\rho^* = 0.3215$, and (d) $\rho^* = 0.3773$. Data are shown for different values of the relative surface area of the perturbation. The circles correspond to the results obtained from perturbations with $\xi > 0$ (increasing-area, γ^{+*}), the squares to the data for perturbations with $\xi < 0$ (decreasing-area, γ^{-*}), and the diamonds to the data from combined increasing/decreasing surface area (central difference scheme given by Eq. (11), γ^*). The error bars are larger than the vertical scale of figure and are not shown for clarity.

$\rho^* = 0.3773$ to 0.6431. In fact, the SF interfacial tension increases (i.e., it becomes less negative) a 2.6% approximately for the system with $r_c^* = 4.5$ and about a 1.3% for that with $r_c^* = 2.5$, as can be seen in Table I. How is it possible to explain this behaviour? Actually, the explanation of the presence of this minimum in the SF interfacial tension, as a function of density inside the cylinder, is also related with the competition between the fluid-fluid and solid-fluid cohesive energies

TABLE I. Interfacial tension for the SF interface in systems of LJ molecules with fluid-fluid cutoff distance of (a) $r_c^* = 4.5$ and (b) $r_c^* = 2.5$ adsorbed on cylindrical pores with two different radii as obtained by a linear extrapolation to $|\xi| \to 0$ of the values obtained from increasing-area (γ^{+*}) and decreasing-area (γ^{-*}) perturbations, and a combined increasing-decreasing (γ^*) perturbation given by Eq. (11) in MC *NVT* simulations at reduced temperature $T^* = 2.0$, and different reduced densities and system sizes.

ρ^*	$\gamma_{(a)}^{+*}$	$\gamma_{(a)}^{-*}$	$\gamma_{(a)}^{*}$	$\gamma_{(b)}^{+*}$	$\gamma_{(b)}^{-*}$	$\gamma_{(b)}^{*}$
			$R^* = 7.5\ N = 500$			
0.1886	− 1.717(7)	− 1.717(7)	− 1.718(5)	− 1.74(2)	− 1.74(2)	− 1.740(6)
0.2829	− 2.36(3)	− 2.36(3)	− 2.36(2)	− 2.40(3)	− 2.40(2)	− 2.40(2)
0.3215	− 2.563(7)	− 2.563(7)	− 2.563(5)	− 2.61(2)	− 2.61(2)	− 2.603(7)
0.3773	− 2.77(3)	− 2.77(3)	− 2.77(2)	− 2.81(2)	− 2.82(2)	− 2.81(2)
0.6431	...	...	...	...	...	...
			$R^* = 7.5\ N = 1000$			
0.1886	− 1.717(5)	− 1.718(5)	− 1.718(4)	− 1.737(4)	− 1.739(5)	− 1.737(3)
0.2829	− 2.360(5)	− 2.360(6)	− 2.360(4)	− 2.40(3)	− 2.40(3)	− 2.40(2)
0.3215	− 2.551(7)	− 2.553(7)	− 2.55(2)	− 2.59(2)	− 2.59(2)	− 2.59(7)
0.3773	− 2.78(2)	− 2.78(2)	− 2.779(7)	− 2.820(7)	− 2.820(2)	− 2.819(6)
0.6431	− 2.71(5)	− 2.71(5)	− 2.71(3)	− 2.78(4)	− 2.78(4)	− 2.78(3)
			$R^* = 5.0\ N = 500$			
0.3778	− 2.594(6)	− 2.594(5)	− 2.594(5)	− 2.63(2)	− 2.632(7)	− 2.635(6)
0.6366	− 2.24(4)	− 2.25(3)	− 2.25(3)	− 2.36(3)	− 2.36(3)	− 2.36(3)

involved in this problem. According to our previous explanation for the variation of the surface tension with density inside the cylinder, if density is increased the solid-fluid cohesive energy of the system increases relatively with respect to the fluid-fluid cohesive energy. This can be clearly understood by a simple inspection of Fig. 1(a): most of the molecules, at low densities, are adsorbed preferentially close to the curved surface of the cylinder. As the density increases, additional layers of adsorbed molecules appear closer to the center of the cylinder. As the number of layers is increased, the rate at which the SF interfacial tension becomes more negative decreases, although the absolute value of γ increases (see Table I). However, when density inside the cylinder changes from 0.3773 to 0.6431, the system seems to exhibit a pronounced pore filling. Due to that, the density in the central part of the cylinder is greatly enhanced (see Fig. 1(a)), and as a consequence of this, the fluid-fluid interactions become relatively more important than the solid-fluid interactions, leading to an effective decrease of the solid-fluid cohesive energy producing the increase of the SF interfacial tension observed in our simulations. This explanation is also corroborated with the values obtained for the LJ system with a cutoff distance of $r_c^* = 2.5$. For this system, the increase of SF interfacial tension is lower when passing from $\rho^* = 0.3773$ to 0.6431, which is a direct consequence of the lower fluid-fluid cohesive energies in comparison with those in systems with $r_c^* = 4.5$.

It is important to note that the calculation of the SF interfacial is, in general, less sensitive to molecular details than the fluid-fluid surface tension of similar models. In particular, the fluctuations of the γ values, as well as the estimation of the errors, are much smaller than that in the case of free interfaces. As in previous works,[24,58] if the size of the perturbation is larger, the values of the interfacial tension computed using the surface area perturbation with a forward or backward difference scheme deviate systematically from the extrapolate values shown in Fig. 2 and Table I.

In order to investigate the effect of system size on the interfacial tension, we have also considered systems formed by $N = 1000$ LJ molecules, at the same thermodynamic conditions and confined in the same geometry. In this case, the length of the simulation box along the z-axis is set equal to $L_z^* = 30$ ($\rho^* = 0.1886$), $L_z^* = 20$ ($\rho^* = 0.2829$), $L_z^* = 17.6$ ($\rho^* = 0.3215$), $L_z^* = 15$ ($\rho^* = 0.3773$), and $L_z^* = 8.8$ ($\rho^* = 0.6431$). Results corresponding to systems formed by $N = 1000$ LJ molecules are shown in Table I. Note that the results for the higher density studied for $R^* = 7.5$ and $N = 1000$ are not represented in Fig. 3 because they exhibit the same behaviour as those corresponding to lower densities already shown in the figure. As can be seen, the SF interfacial tension is nearly independent of the system size, an issue that we have checked in all the simulations we have performed.

We have also calculated the SF interfacial tension of the LJ molecules, but now with a cutoff distance $r_c^* = 2.5$, at the same temperature and densities considered for the cylindrical pore of radius $R^* = 7.5$. The results obtained from our simulations are shown in Fig. 3 and Table I. Here we do not discuss the effect of the system size on interfacial tension because, as previously mentioned, is qualitatively identical than those corresponding to the case of $r_c^* = 4.5$. As can be seen,

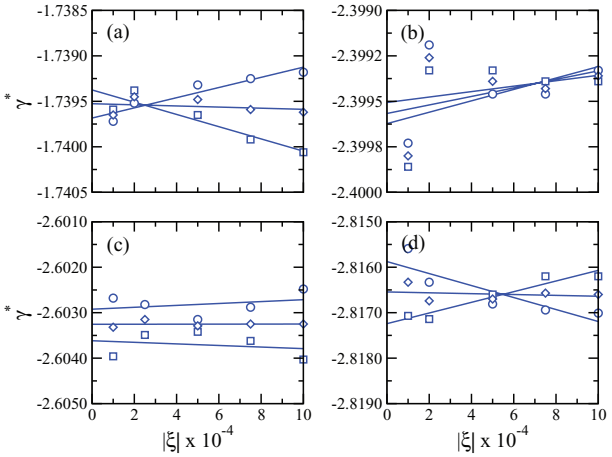

FIG. 3. Interfacial tension for the SF interface in a system of $N = 500$ LJ molecules adsorbed on a cylindrical pore of radius $R^* = 7.5$ as obtained from surface area perturbations in MC *NVT* simulations with fluid-fluid interaction cutoff distance at $r_c^* = 2.5$. The reduced temperature is $T^* = 2.0$ and density inside the cylindrical pore is (a) $\rho^* = 0.1886$, (b) $\rho^* = 0.2829$, (c) $\rho^* = 0.3215$, and (d) $\rho^* = 0.3773$. The meaning of data is the same as in Fig. 2.

the data exhibit now a strong dependence on the size and sign of the relative SF surface area change $\xi = \Delta\mathcal{A}/\mathcal{A}$. A similar behaviour was also observed by de Miguel and Jackson[24] when the cutoff distance was decreased. However, the extrapolated values obtained for the SF interfacial tension in the case $r_c^* = 2.5$ as $|\xi| \to 0$ are very similar than those corresponding to systems in which $r_c^* = 4.5$, as can be seen in Table I. In fact, differences between both results (for all densities considered) are less than a 2% in all cases. As in the case of the LJ system with $r_c^* = 4.5$, a small but measurable dependence on density is also observable. In addition to that, the SF interfacial tension values corresponding to the case $r_c^* = 2.5$ are systematically more negative than those corresponding to $r_c^* = 4.5$. This may be explained in terms of the behaviour of the cohesion energy of the system when varying the cutoff distance. The attractive forces between LJ molecules with shorter cutoff distances are weaker than those associated to larger r_c values. Due to that, the SF cohesive energy of the system effectively increases, leading to a more negative SF interfacial tension. It is important to recall again that although the differences are measurables, as Monte Carlo simulations indicate, from a practical point of view they are negligible.

Finally, and in order to check the ability of the method for calculating the SF interfacial tension in narrower pores, we consider now the behaviour of $N = 500$ LJ molecules, using two different fluid-fluid cutoff distances, $r_c^* = 4.5$ and 2.5, inside a thinner cylindrical pore of radius $R^* = 5.0$ at the same reduced temperature, $T^* = 2.0$. We study only two different densities, $\rho^* = 0.3778$ (with $L_z^* = 16.85$) and 0.6366 (with $L_z^* = 10$). Figures 4(a) and 4(b) show the behaviour of the interfacial tension (using increasing-area, decreasing-area, and central difference scheme) as a function of the relative SF surface change $|\xi|$. As can be seen in Fig. 4(a), the SF interfacial tension also exhibits a definite linear behaviour over the range of values of ξ considered in this work. The behaviour observed for the interfacial tension, as a function of

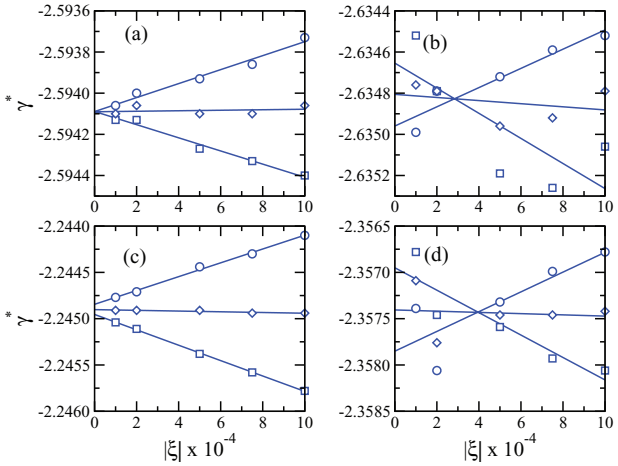

FIG. 4. Interfacial tension for the SF interface in a system of $N = 500$ LJ molecules adsorbed on a cylindrical pore of radius $R^* = 5.0$ as obtained from surface area perturbations in MC *NVT* simulations at reduced temperature $T^* = 2.0$ and different densities and fluid-fluid interaction cutoff distances: (a) $\rho^* = 0.3778$ and $r_c^* = 4.5$, (b) $\rho^* = 0.3778$ and $r_c^* = 2.5$, (c) $\rho^* = 0.6366$ and $r_c^* = 4.5$, and (d) $\rho^* = 0.6366$ and $r_c^* = 2.5$. The meaning of data is the same as in Fig. 2.

ξ, is smoother and more uniform in the case of the LJ systems with the larger cutoff distance. This behaviour is in agreement with the results from de Miguel and Jackson[24] and with the results previously shown here for the case of the cylindrical pore with radius $R^* = 7.5$. Data values obtained from linear fits and extrapolation procedure as $|\xi| \to 0$ are also presented in Table I. As can be seen in part (b) of the figure, the SF interfacial tension values of the LJ system with $r_c^* = 2.5$ is more negative, a 4%–5% approximately, than those corresponding to the system with $r_c^* = 4.5$. This result is in agreement with our previous argument by which a LJ system with shorter cutoff distance ($r_c^* = 2.5$) exhibits weaker attractive interactions, and consequently, the SF cohesive energy is enhanced compared with a system with larger values of the cutoff distance ($r_c^* = 4.5$). In our particular case, as can be seen in Table I, this provokes larger negative values in the corresponding SF tension for the case of $r_c^* = 2.5$.

As in the case of the widest cylindrical pore, $R^* = 7.5$, the SF interfacial tension of LJ molecules inside the pore of $R^* = 5.0$ increases (it becomes less negative) when passing from a density of $\rho^* = 0.3778$–0.6366 (see Table I and Figs. 4(c) and 4(d)). The reason of this behaviour has been explained previously, although now the effect is more important. In the case of LJ molecules absorbed in a cylinder of radius $R^* = 7.5$, the increase of the SF interfacial tension (γ becomes less negative) is approximately a 2.6% in the case of fluids with $r_c^* = 4.5$ and a 1.3% in those with $r_c^* = 2.5$. As can be seen in Table I, the increase of the SF interfacial tension in the cylinder with $R^* = 5.0$ is a 13% and 10% for fluids with $r_c^* = 4.5$ and $r_c^* = 2.5$, respectively. The enhancement of this effect when passing from a cylindrical pore of $R^* = 7.5$ to other thinner ($R^* = 5.0$) is because the narrower pore is more adsorbent than the other one. As it was discussed previously, the effect of the local confinement in the narrower pore, at the same total density inside de cylinder, is higher compared with that of the wider pore. This effect, that it is clearly seen in Figs. 1(a) and 1(b), and particularly, when comparing the structure of the confined fluids in the center of the pores, explains the increasing of the difference between the fluid-fluid and solid-fluid cohesive energies, and hence, the behaviour observed in our computer simulation results.

V. CONCLUSIONS

We have extended the TA methodology, originally proposed to evaluate the surface tension of vapour-liquid interfaces along a computer simulation in the canonical ensemble, to calculate the solid-fluid interfacial tension of systems adsorbed on cylindrical pores. This has been done following the original work of Gloor *et al.* and performing free-energy perturbations due to virtual changes in the solid-fluid surface area. In particular, the method allows one to modify appropriately the radius and length of the cylindrical pore by ensuring constant-volume virtual changes along the simulation. According to this, we perform both increasing and decreasing surface area perturbations to very accurately account for the value of the solid-fluid interfacial tension as long as the magnitude of the perturbation is small enough or if values are extrapolated to $\xi = |\Delta\mathcal{A}|/\mathcal{A} \to 0$, where $\Delta\mathcal{A}$ is relative change of surface area. We also combine increasing-decreasing perturbations to estimate the surface area with a central finite-difference approximation, allowing to obtain very accurate values of the solid-fluid interfacial tension.

We have applied the new methodology performing canonical Monte Carlo computer simulations to calculate the solid-fluid interfacial tension of spherical molecules (that interact through the Lennard-Jones intermolecular potential) adsorbed in cylindrical pores with different pore sizes, densities of adsorbed molecules, and fluid-fluid cutoff distances of the Lennard-Jones intermolecular potential. Solid-fluid interactions are accounted for the generalization of the well-known 10-4-3 Steele potential for cylindrical pores recently proposed by Siderius and Gelb. Results indicate that an increase of the density of adsorbed molecules inside the pore provokes more negative solid-fluid interfacial tension values. This effect is the result of a competition between the solid-fluid and fluid-fluid cohesive energies. However, at the highest densities considered, the effect is inverted. This can be explained taking into account the existence of a phase transition that occurs at high densities. Since above the coexistence density the system seems to exhibit a liquid-like phase inside the pore (and not a gas-like phase as it occurs at lower densities), the fluid-fluid cohesive energy is enhanced, in comparison with the solid-fluid cohesion, provoking a change in the behaviour of the interfacial tension as a function of density. Finally, the effect of fluid-fluid cutoff distance associated to the Lennard-Jones intermolecular interactions on the solid-fluid interfacial tension is usually negligible, although it can be more important in the case of small cylindrical pores.

It is important to note that the solid-fluid interfacial tension, for a particular pressure, must be a function of the cylindrical radius. In particular, γ^* must approach asymptotically to a solid-fluid interfacial value of a planar system comparable to the cylindrical system. Since the goal of this work

is to generalize the TA technique to deal with the interfacial tension of systems confined in cylindrical pores, we have not performed a systematic study of the behaviour of γ^* with the cylindrical radius and its comparison with equivalent planar systems. This will be the subject of a future work.

ACKNOWLEDGMENTS

The authors would like to acknowledge helpful discussions with A. I. Moreno-Ventas Bravo, M. M. Piñeiro, and J. M. Míguez. This work was supported by Acción Integrada España-Francia from Ministerio de Ciencia e Innovación and Picasso Project (Project Nos. FR2009-0056 and PHC PICASSO2010). Further financial support from Proyecto de Excelencia from Junta de Andalucía (Project No. P07-FQM02884), Ministerio de Ciencia e Innovación (Project No. FIS2010-14866), and Universidad de Huelva are also acknowledged.

[1] J. W. Cahn and J. E. Hilliard, J. Chem. Phys. **28**, 258 (1958).
[2] B. S. Carey, H. T. Davis, and L. E. Scriven, AIChE J. **26**, 705 (1980).
[3] C. Miqueu, B. Mendiboure, A. Graciaa, and J. Lachaise, Fluid Phase Equilib. **218**, 189 (2004).
[4] C. Miqueu, B. Mendiboure, A. Graciaa, and J. Lachaise, Ind. Eng. Chem. Res. **44**, 3321 (2005).
[5] G. Galliero, M. M. Piñeiro, B. Mendiboure, C. Miqueu, T. Lafitte, and D. Bessières, J. Chem. Phys. **130**, 104704 (2009).
[6] T. Lafitte, B. Mendiboure, M. M. Piñeiro, D. Bessières, and C. Miqueu, J. Phys. Chem. B **114**, 11110 (2010).
[7] C. Miqueu, J. M. Míguez, M. M. Piñeiro, T. Lafitte, and B. Mendiboure, J. Phys. Chem. B **115**, 9618 (2011).
[8] R. Evans, "Density functionals in the theory of nonuniform fluids," in *Fundamentals of Inhomogeneous Fluids* (Dekker, New York, 1992).
[9] H. T. Davis, *Statistical Mechanics of Phases, Interfaces and Thin Films* (VCH, Weinhem, 1996).
[10] Y. Rosenfeld, Phys. Rev. Lett. **63**, 980 (1989).
[11] Y. X. Yu and J. Z. Wu, J. Chem. Phys. **117**, 2368 (2002).
[12] Y. X. Yu and J. Z. Wu, J. Chem. Phys. **119**, 2288 (2003).
[13] F. Llovell, A. Galindo, F. J. Blas, and G. Jackson, J. Chem. Phys. **133**, 024704 (2010).
[14] A. Malijevský and G. Jackson, J. Phys. Condens. Matter **24**, 464121 (2012).
[15] J. H. Irving and J. G. Kirkwood, J. Chem. Phys. **18**, 817 (1950).
[16] A. Harasima, Adv. Chem. Phys. **1**, 203 (1958).
[17] M. P. Allen, J. Chem. Phys. **124**, 214103 (2006).
[18] E. de Miguel and G. Jackson, Mol. Phys. **104**, 3717 (2006).
[19] P. E. Brumby, A. J. Haslam, E. de Miguel, and G. Jackson, Mol. Phys. **109**, 169 (2011).
[20] J. R. Errington and D. A. Kofke, J. Chem. Phys. **127**, 174709 (2007).
[21] E. de Miguel, J. Phys. Chem. B **112**, 4674 (2008).
[22] L. G. MacDowell and P. Bryk, Phys. Rev. E **75**, 061609 (2007).
[23] G. J. Gloor, G. Jackson, F. J. Blas, and E. de Miguel, J. Chem. Phys. **123**, 134703 (2005).
[24] E. de Miguel and G. Jackson, J. Chem. Phys. **125**, 164109 (2006).
[25] F. J. Blas, L. G. MacDowell, E. de Miguel, and G. Jackson, J. Chem. Phys. **129**, 144703 (2008).
[26] F. J. Blas, F. J. Martínez-Ruiz, A. I. M.-V. Bravo, and L. G. MacDowell, J. Chem. Phys. **137**, 024702 (2012).
[27] F. J. Blas, A. I. M.-V. Bravo, J. M. Míguez, M. M. Piñeiro, and L. G. MacDowell, J. Chem. Phys. **137**, 084706 (2012).
[28] C. Vega and E. de Miguel, J. Chem. Phys. **126**, 154707 (2007).
[29] J. M. Míguez, D. González-Salgado, J. L. Legido, and M. M. Piñeiro, J. Chem. Phys. **132**, 184102 (2010).
[30] J. M. Míguez, M. M. Piñeiro, and F. J. Blas, J. Chem. Phys. **138**, 034707 (2013).
[31] P. Orea, Y. Reyes-Mercado, and Y. Duda, Phys. Lett. A **372**, 7024 (2008).
[32] E. de Miguel, N. G. Almarza, and G. Jackson, J. Chem. Phys. **127**, 034707 (2007).
[33] F. Biscay, A. Ghoufi, F. Goujon, V. Lachet, and P. Malfreyt, J. Chem. Phys. **130**, 184710 (2009).
[34] J. R. Henderson and F. van Swol, Mol. Phys. **51**, 991 (1984).
[35] M. Heni and H. Löwen, Phys. Rev. E **60**, 7057 (1999).
[36] F. Varnik, J. Baschnagel, and K. Binder, J. Chem. Phys. **113**, 4444 (2000).
[37] A. Fortini, M. Dijkstra, M. Schmidt, and P. P. F. Wessels, Phys. Rev. E **71**, 051403 (2005).
[38] Y. Hamada, K. Koga, and H. Tanaka, J. Chem. Phys. **127**, 084908 (2007).
[39] J. K. Singh and S. K. Kwak, J. Chem. Phys. **126**, 024702 (2007).
[40] S. K. Das and K. Binder, Mol. Phys. **109**, 1043 (2011).
[41] L. D. Gelb, K. E. Gubbins, R. Radhakrishnan, and M. Sliwinska-Bartkowiak, Rep. Prog. Phys. **62**, 1573 (1999).
[42] L. A. del Pino, A. L. Benavides, and A. Gil-Villegas, Mol. Simul. **29**, 345 (2003).
[43] R. Evans, J. Phys. Condens. Matter **2**, 8989 (1990).
[44] J. M. Míguez, M. M. Piñeiro, A. I. M.-V. Bravo, and F. J. Blas, J. Chem. Phys. **136**, 114707 (2012).
[45] R. Lovett and M. Baus, J. Chem. Phys. **106**, 635 (1997).
[46] M. Mareschal, M. Baus, and R. Lovett, J. Chem. Phys. **106**, 645 (1997).
[47] R. Lovett and M. Baus, J. Chem. Phys. **120**, 10711 (2004).
[48] S. M. Thompson, K. E. Gubbins, J. P. R. B. Walton, R. A. R. Chantry, and J. S. Rowlinson, J. Chem. Phys. **81**, 530 (1984).
[49] S. Figueroa-Gerstenmaier, F. J. Blas, J. B. Avalos, and L. F. Vega, J. Chem. Phys. **118**, 830 (2003).
[50] A. Malijevský, J. Chem. Phys. **126**, 134710 (2007).
[51] R. Eppenga and D. Frenkel, Mol. Phys. **52**, 1303 (1984).
[52] V. I. Harismiadis, J. Vorholz, and A. Z. Panagiotopoulos, J. Chem. Phys. **105**, 8469 (1996).
[53] F. Biscay, A. Ghoufi, and P. Malfreyt, J. Phys. Chem. B **134**, 044709 (2011).
[54] D. W. Siderius and L. D. Gelb, J. Chem. Phys. **135**, 084703 (2011).
[55] W. A. Steele, *The Interaction of Gases with Solid Surfaces* (Pergamon, 1974).
[56] M. G. Martin and J. I. Siepmann, J. Phys. Chem. B **102**, 2569 (1998).
[57] D. Frenkel and B. Smit, *Understanding Molecular Simulation* (Academic Press, 2002).
[58] J. G. Sampayo, A. Malijevský, E. A. Müller, E. de Miguel, and G. Jackson, J. Chem. Phys. **132**, 141101 (2010).